

Fig. 4 Fence effectiveness as a function of gap ratio.

where  $C_{L\alpha}(0)$  is the lift curve slope for infinite fence (zero gap),  $C_{L\alpha}(0.1, g)$  corresponds to the fence height ratio  $h/(h + s) = 0.1$  and a given value of  $g/(g + s)$ , and  $C_{L\alpha}(0, g)$  applies to zero fence height but the same value of gap ratio. The closer  $F_e$  is to unity the more effective the fence.

Using Fig. 3, a choice can be made of a root fence size that is compatible with the experimental error likely in a particular situation. A minimization of fence dimensions is therefore possible.

References

- <sup>1</sup> Bleviss, Z. O. and Strubble, R. A., "Some Aerodynamic Effects of Streamwise Gaps in Low Aspect Ratio Lifting Surfaces at Supersonic Speeds," *Journal of the Aeronautical Sciences*, Vol. 21, No. 10, Oct. 1954, pp. 665-674.
- <sup>2</sup> Dugan, D. W. and Hikido, K., "Theoretical Investigation of the Effects upon Lift of a Gap Between Wing and Body of a Slender Wing-Body Combination," TN 3224, 1954, NACA.
- <sup>3</sup> Judd, M., "The Effect of a Root Gap on the Aerodynamic Forces of a Slender Delta Wing in Oscillatory Pitching Motion," *The Aeronautical Quarterly*, Vol. XIV, No. 3, Aug. 1963, pp. 299-310.
- <sup>4</sup> Glauert, H., *The Elements of Aerofoil and Airscrew Theory*, 2nd ed., Cambridge University Press, Cambridge, England, 1948, p. 173.

## Spectroscopically Measured Velocity Profiles of an MPD Arcjet

M.-U. BETH\* AND M. G. KLING\*

*Deutsche Forschungs- und Versuchsanstalt für Luft- und Raumfahrt, Institut für Plasmadynamik, Stuttgart-Vaihingen, West Germany*

DETAILED comprehension of the physical processes in a plasma jet, for instance the mechanism of acceleration, departures from thermodynamic equilibrium, or dissipation of energy, requires information on spatial resolved plasma parameters. For this purpose, the plasma jet was investigated with respect to the Doppler shift of spectral lines resulting from macroscopic velocities in axial and rotational directions. Certainly many recent papers<sup>1-4</sup> dealt with spectroscopic measurements of arcjet velocities, but to our knowledge no profiles of local velocities were obtained.

Received July 16, 1969. The authors are indebted to P. Tattermusch for useful and active technical assistance.

\* Diplomphysiker.

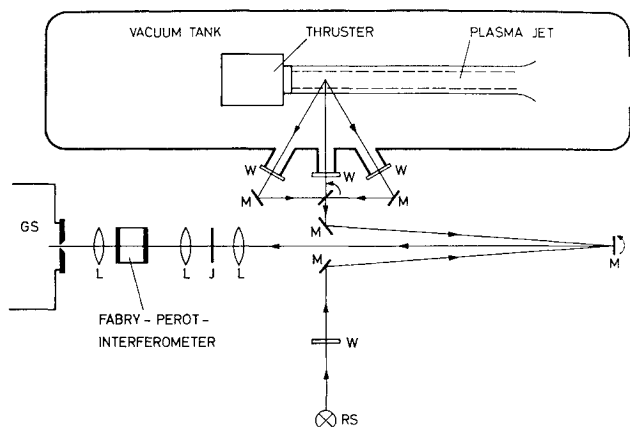


Fig. 1 Optical arrangement, schematic: W = window, M = mirror, RS = radiation standard, L = lens, J = image plane, and GS = grating spectrograph.

### The Plasma Jet

The plasma jet was generated by a continuous MPD arc thruster<sup>5</sup> under the following conditions: 650-amperes arc current, 40-v arc voltage, 1000-gauss external magnetic field at the cathode tip, 0.22-g/sec argon mass flow, and 0.76-torr background pressure. The off-axis intensity of a spectral line was recorded and observed on an oscilloscope in order to secure reproducibility and no spoke mode operation.

### Optical Arrangement

The optical arrangement, see Fig. 1, was chosen in a manner such that the plasma jet was imaged by an achromatic and two telephoto lenses in two steps on the slit (slit width 0.03 cm) of a 2-m plane grating spectrograph. An intermediate image was performed at J, and a Perot-Fabry interferometer of 0.2-cm etalon distance was adjusted between the two telephoto lenses in order to superpose a system of interference fringes on each spectral line. Using this arrangement, both a sufficient spatial and high wavelength-resolution was reached in one dimension, i.e., the slit direction. By interchanging mirrors, optional side-on or angle-on views of the plasma jet could be imaged. Different sections of the latter were observed by displacing the thruster as shown in Fig. 2.

### Measurements

Measurements of integrated Doppler shifts along the line of sight originating from plasma rotation have been performed at each section, I, II and III, see Fig. 2, by taking two interferograms with opposite directions of magnetic field and thus changed sense of rotation. The line shifts were obtained photometrically from the photo plate by comparing the distances between homologous fringes in the two interferograms and an exact reproducible marking that was produced by imaging a narrow cross slit with continuous light in each spectrum on the photo plate. (This method differs from that applied in a paper,<sup>6</sup> previously published by the authors, the results of which seem to be doubtful in the light of recent experiments.) The integrated Doppler shifts with respect to

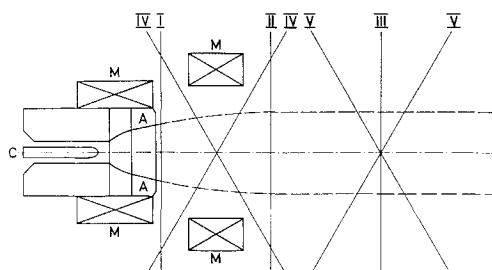


Fig. 2 Thruster and investigated sections, schematic: C = cathode, A = Anode, and M = magnetic coil.

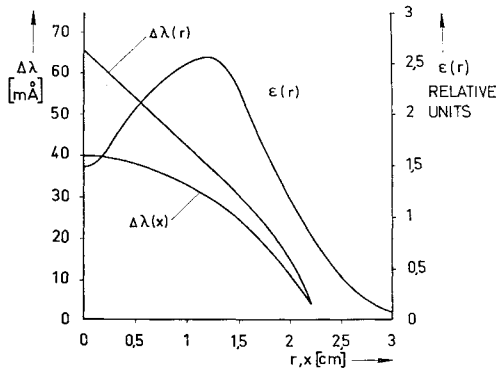


Fig. 3 Measured and transformed Doppler shifts.

the axial velocity of the plasma jet were measured at Secs. IV and V (Fig. 2) in a manner similar to the one mentioned previously. The two interferograms, however, were taken upstream and downstream, respectively, at an angle of 60° against the axis of the plasma jet, thus experimentally eliminating the rotational parts of the line shifts as a first-order approximation. Profiles of relative intensities which were additionally required, as will be shown below, were measured at each section in question by removing the interferometer from the light path. Since spectral lines of neutral argon have not been observed, the Doppler shifts were obtained from lines of singly ionized argon, especially from the line at 4348 Å.

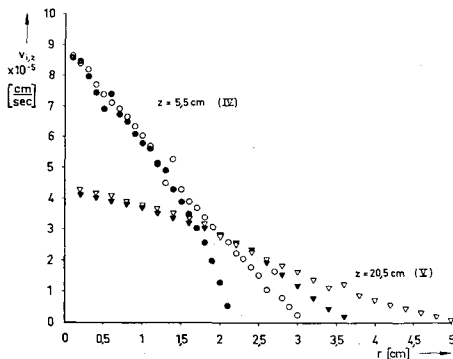


Fig. 4 Axial velocity profiles at Secs. IV and V.

Transformation

The transformation of the measured gross Doppler shift profiles to local quantities has been accomplished by using the intensity profiles and profiles of emission coefficients computed from these via an Abel transform as weights in a modified Abel transform for rotational and elliptical cases. Figure 3 shows profiles of integrated Doppler shifts, emission coefficients, and transformed local Doppler shifts; the utility of the transform is evident, especially if the profiles of the emission coefficient flatten in the region near the axis. If the geometry of the jet deviates considerably from cylinder symmetry, the accuracy of the results of the transform decreases with increasing radius.

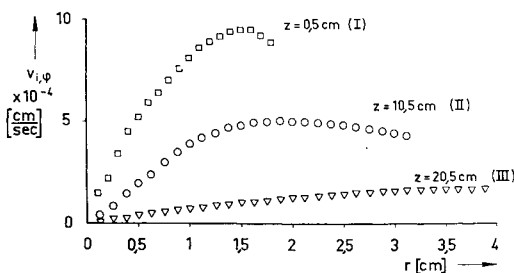


Fig. 5 Rotational velocity profiles at Secs. I, II, and III.

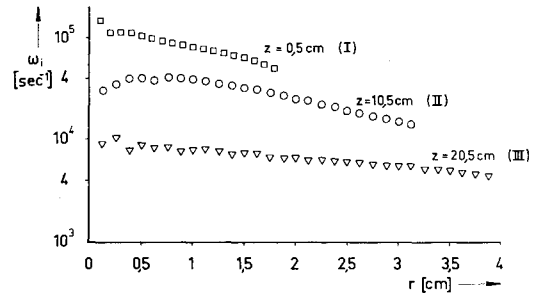


Fig. 6 Angular frequency of the jet vs radius at Secs. I, II, and III.

Results

Figures 4-6 show the profiles of axial and rotational velocity and the angular frequency, Fig. 6 illustrating the non-rigid-body rotation of the jet. A detailed description of experimental methods and transformation formulas may be found in previously published papers.<sup>6,7</sup>

References

- <sup>1</sup> Kogelschatz, U., "Doppler Shift Measurements of Axial and Rotational Velocities in an MPD Arc," AIAA Paper 69-110, New York, 1969; also *AIAA Journal*, to be published.
- <sup>2</sup> Malliaris, A. C. and Libby, D. R., "Velocities of Neutral and Ionic Species in an MPD Flow," AIAA Paper 69-109, New York, 1969.
- <sup>3</sup> Fradkin, D. B. et al., "Experiments Using a 25 kW Hollow Cathode Lithium Vapor MPD Arc Jet," AIAA Paper 69-241, Williamsburg, Va., 1969; also *AIAA Journal*, to be published.
- <sup>4</sup> Connolly, D. J. and Sovie, R. J., "The Effect of Background Pressure and Magnetic Field Shape on MPD Thruster Performance," AIAA Paper 69-243, Williamsburg, Va., 1969.
- <sup>5</sup> Krülle, G., "Characteristics and Local Analysis of MPD Thruster Operation," AIAA Paper 67-672, Colorado Springs, Colo., 1967.
- <sup>6</sup> Beth, M.-U. et al., "Angular Velocity Profiles of a Rotating Argon Plasma Jet," Paper 6.2.4., VIIIth International Conference on Phenomena in Ionized Gases, Vienna, 1967.
- <sup>7</sup> Bohn, W. L., Beth, M.-U., and Nedder, G., "On Spectroscopic Measurements of Velocity Profiles and Non-Equilibrium radial Temperatures in an Argon Plasma Jet," *Journal of Quantitative Spectroscopy and Radiative Transfer*, Vol. 7, 1967, pp. 661-676.

A Numerical Solution of the Conduction Problem with Radiating Surface

CAROLYN MASON\*

McDonnell Douglas Astronautics Company, Santa Monica, Calif.

Nomenclature

- Q = surface heat flux
- c<sub>p</sub> = specific heat
- ρ = density
- t = time
- h = distance
- K = thermal conductivity
- α = thermal diffusivity
- T = temperature
- ε = emissivity

Received April 16, 1969; revision received July 15, 1969. This work was supported by the MDAC-WD Independent Research and Development Program.

\* Computing Engineer, Information Processing System Department, Western Division.